Dendrochronologia 73 (2022) 125958

Contents lists available at ScienceDirect

Dendrochronologia

journal homepage: www.elsevier.com/locate/dendro

The temperature sensitivity along elevational gradients is more stable in maximum latewood density than tree-ring width

Claudia Hartl [a,*], Lea Schneider [b], Dana F.C. Riechelmann [c], Eileen Kuhl [d], Markus Kochbeck [d], Lara Klippel [e], Ulf Büntgen [f,g,h], Jan Esper [d,h]

[a] *Nature Rings – Environmental Research and Education, Mainz, Germany*
[b] *Department of Geography, Justus-Liebig-University, Gießen, Germany*
[c] *Institute for Geosciences, Johannes Gutenberg University, Mainz, Germany*
[d] *Department of Geography, Johannes Gutenberg University, Mainz, Germany*
[e] *Deutscher Wetterdienst, Offenbach, Germany*
[f] *Department of Geography, University of Cambridge, UK*
[g] *Swiss Federal Research Institute WSL, Birmensdorf, Switzerland*
[h] *Global Change Research Centre AS CR, Brno, Czech Republic*

ARTICLE INFO

Keywords:
Abiotic site factors
European Alps
Climate sensitivity
Dendroecology
Dendroclimatology
European larch

ABSTRACT

Tree ring-based temperature reconstructions are preferably derived from maximum latewood density (MXD) compared to tree-ring width (TRW). Although temperature signals in MXD are less dependent on site ecology, systematic analyses of the effects of elevation and slope aspect on ring formation are still lacking. Here, we assess the climate sensitivity of MXD and TRW chronologies from six larch (*Larix decidua* Mill.) sites across the Simplon valley in the southwestern Swiss Alps, representing elevations from 1400 to 2150 m asl on both north- and south-facing slopes. We find decreasing temperature signals with decreasing elevation in MXD and TRW, though correlation coefficients are generally higher for MXD and on the warmer and dryer south exposed slopes. While the greatest temperature signals are found for MJJA at highest elevations with $r = 0.71$ for MXD and $r = 0.57$ for TRW (both $p < 0.05$ and for the 1928–2009 common period), MXD still correlates significantly positive at the lowest elevation site that is ~750 m below the treeline. Our findings indicate the suitability of MXD over TRW for temperature reconstructions when using historical wood sources of unknown origin.

1. Introduction

For Europe, more than a dozen tree-ring based temperature reconstructions exist, which span at least the past millennium (see Esper et al., 2016 for an overview). These reconstructions are, however, clustered over a few regions that meet the requirements for the development of a robust temperature reconstruction: i) a strong temperature signal fingerprinted in the tree-rings, and ii) sample availability covering this time scale (Hartl et al., 2021). Potential sites are thus restricted to regions where tree growth is temperature limited, i.e. elevational or latitudinal treeline sites, and additionally suitable material is present (Hartl et al., 2021).

In order to enhance a weak temperature signal in tree-rings from lower elevations it is suggested to use maximum latewood density (MXD) instead of tree-ring width (TRW) as tree-ring proxy (Frank and Esper, 2005). It is also expected that MXD data is generally less biased by site-ecology and thus more suitable for climate reconstructions. Björklund et al. (2019) even described "MXD as the current gold standard of high-resolution palaeoclimatology for temperature reconstructions", due to the many advantages MXD has over TRW.

Europe was strongly affected by intense land-use (changes), including deforestation and high population densities (Duffy et al., 2019; Luterbacher et al., 2016) causing the removal of many old trees. Therefore, living trees usually do not reach millennial age (except of two known scientifically dated examples, "*Adonis* "(Konter et al., 2017) and "*Italus*" (Piovesan et al., 2018)) meaning that relict or historical material has to be used to extend a chronology back in time.

Various MXD-based temperature reconstructions have been produced for the last several centuries in Europe with in situ material. In Northern Europe, such samples are available as logs preserved in lakes

* Corresponding author.
E-mail address: info@claudia-hartl.com (C. Hartl).

https://doi.org/10.1016/j.dendro.2022.125958
Received 16 October 2021; Received in revised form 26 March 2022; Accepted 31 March 2022
Available online 9 April 2022

or subterrestrial (Esper et al., 2012; Schweingruber et al., 1988), and in Southern Europe temperature reconstructions were produced with dead wood lying on the ground in Greece (Esper et al., 2020a; Klippel et al., 2019), with a combination of water logs and dead wood in the Pyrenees (Büntgen et al., 2017) or – in a few places – with living trees only (Esper et al., 2020b; Römer et al., 2021). For Eastern Europe, there also exists a temperature reconstruction in the Tatra Mountains (Büntgen et al., 2013) and for Central Europe in the European Alps (Büntgen et al., 2005; Schweingruber et al., 1988), but for the development of the underlying chronologies, timber from historical buildings were used. In the humid climate of Central Europe relict material can resist decomposition only if water or sediments impede gas exchange. Few sites match these prerequisites for in situ grown dead wood. The long population histories of Central European mountain areas, however, still provide many opportunities to sample old wood used as timbers in nearby historical buildings.

Historical buildings were usually located in the valley bottom and it is very unlikely that any timber came from lower elevations (Büntgen et al., 2006) but also unlikely that timbers were derived from trees growing at the tree line. This, however, results in a significant elevation difference between the living material from the tree line and the historical material of unknown origin that extends the chronology back into the past. For the Tatra mountains, for example, it has been shown that the historical timbers likely originate from lower elevations, and should not be merged with higher elevation living trees due to differing climate signals (Klippel et al., 2020). An advantage in the European Alps is that villages as the source for historical timber are already located at higher elevations compared to the Tatra mountains meaning that the trees' original growing sites were located in cold environments, where tree growth is temperature limited, so that living tree and historical material could be merged.

Elevation gradients in climate signals from TRW data have been shown for multiple sites and regions in the European Alps (Hartl-Meier et al., 2014a, 2017; Riechelmann et al., 2020). Even site aspect is influential (Hartl-Meier et al., 2014b, 2015). For MXD, some elevation dependent differences were found by Zhang et al. (2015) and Klippel et al. (2020) but the former study refers to subfossil and dead wood only, without the consideration of living trees, and the latter just differed between two elevational belts. A comparison with TRW data is lacking in both. The effects of site factors and differing environmental conditions at local to regional scales on MXD require a comprehensive investigation and systematic analysis and will be introduced with this study.

We here compiled a MXD and TRW network of six *Larix decidua* Mill. sites in a Swiss valley in the European Alps. We sampled along elevational transects between 1400 and 2150 m asl including north and south exposed slopes. We analyse the respective effects of elevation and site aspect on raw MXD and TRW data as well as inherent climate signals to assess if the unknown origin of timber material potentially affects the robustness of a temperature reconstruction.

2. Material and methods

2.1. Study design and chronology building

Tree-ring data from six different stands in the Simplon valley, Switzerland, are used in this study. We sampled two opposing slopes along elevational transects between 1400 and 2150 m asl. Three sites are located at the north-facing slope and three sites at the south-facing slope (Fig. 1, Table 1). During different field campaigns between 2010 and 2012 at each site a minimum of 25 living *L. decidua* trees were cored twice. Sampling was performed using a 5 mm increment borer at breast height and parallel to the slope. Tree-ring width was measured at an accuracy of 0.01 mm using a LINTAB measurement device and TSAP-WIN software (RINNTECH, Germany). The complete dataset is introduced in Riechelmann et al. (2020). For this study a subset of this compilation was used: at each site we selected two cores from 12 trees (i. e. 24 radii) to guarantee a consistent sample replication. The choice of trees aimed at a heterogenous age-structure, including young and old trees, in order to support the application of regional curve standardisation (RCS, Esper et al., 2003). From these 144 samples we measured maximum latewood density (MXD) using DENDRO2003 X-ray microdensitometer (WALESCH, Electronic GmbH, Switzerland) as described in Björklund et al. (2019).

After checking the cross-dating accuracy visually and statistically with COFECHA (Holmes 1983) we standardised the tree-ring series site-by-site using RCS (Esper et al., 2003) but also produced a chronology including all series. RCS detrending potentially preserves low-frequency variability while the biological age trend is removed, thus representing an ideal detrending technique for temperature reconstructions. For a final temperature reconstruction, RCS would require combinations of living and dead trees in a composite chronology or a pruning of long living-tree datasets (Römer et al., 2021). Albeit RCS remains challenging with living-tree data only, our approach with heterogenous age-structure is still the best choice for our research question. However, to enhance the year-to-year variability and for checking the covariance of site chronologies and climate response in the high-frequency domain we also applied 30-yr cubic smoothing spline detrending (Cook and Peters, 1981). The final chronologies were produced using a bi-weight robust mean (Mosteller and Tukey, 1977) and truncated at a minimum replication of five series. The covariance of RCS and 30-yr spline detrended chronologies was assessed with Pearson's correlation coefficients.

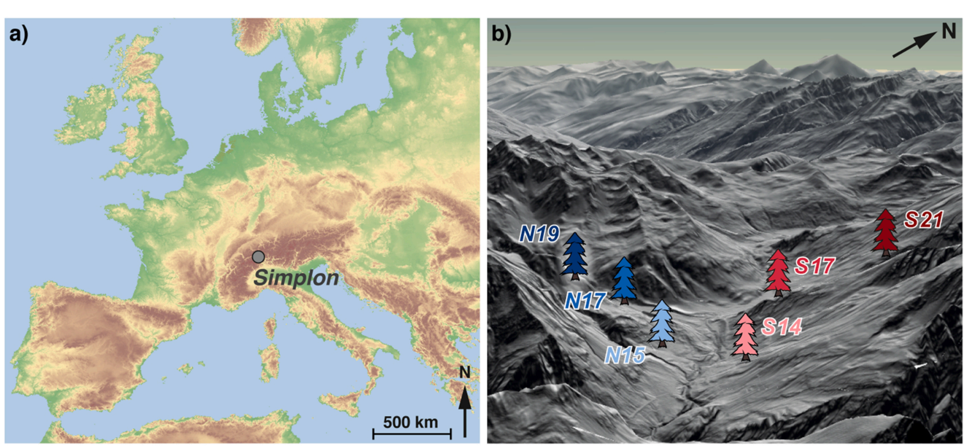

Fig. 1. a) Map showing the location of the Simplon valley in the Swiss Alps and b) the Simplon valley as 3D elevation model with the respective sampling scheme at different elevations and slope aspects. From each site twelve trees, i.e. 24 cores, were used.

Table 1
Characteristics of the maximum latewood density (MXD) and tree-ring width (TRW) chronologies, produced from the same 24 samples at each site. > 5 = First year with replication higher than 5 series, MSL = mean series length, SD = standard deviation, AR1 = first year autocorrelation, EPS = expressed population signal, Rbar = inter-series correlation.

Site	Exposure	Elevation	(First) > 5	Last	MSL	Mean MXD [g/cm³]	Mean TRW [mm]	SD MXD	SD TRW	AR1 MXD	AR1 TRW	EPS MXD	EPS TRW	Rbar MXD	Rbar TRW
S21	south	2150	(1542) 1717	2009	218	0.84	0.73	0.11	0.41	0.52	0.70	0.90	0.93	0.45	0.56
N19	north	1900	(1582) 1685	2010	205	0.90	0.97	0.10	0.43	0.54	0.67	0.88	0.88	0.41	0.41
S17	south	1713	(1641) 1686	2010	170	0.94	0.92	0.13	0.46	0.50	0.76	0.84	0.95	0.30	0.61
N17	north	1712	(1878) 1895	2011	105	0.99	1.15	0.09	0.59	0.41	0.79	0.88	0.97	0.27	0.64
N15	north	1575	(1860) 1870	2011	133	1.02	0.94	0.11	0.57	0.44	0.83	0.90	0.98	0.30	0.67
S14	south	1400	(1884) 1928	2011	73	1.02	1.57	0.09	0.63	0.50	0.68	0.82	0.96	0.23	0.62
All			(1542) 1641	2011	150	0.95	1.29	0.10	0.53	0.48	0.75	0.68	0.85	0.05	0.13

2.2. Statistical analyses

Climate response analyses were performed with bootstrapped correlations of the RCS and 30-yr spline detrended chronologies with previous and current year's temperature and precipitation data (grid 46.125°N 8.125°E, E-OBS v23.1e data, Cornes et al., 2018) for the common period 1928–2009. Additional spatial correlations were calculated with Pearson's correlation coefficients and mean May/June/July/August (MJJA) temperature. We used linear regression models to assess the influence of elevation on raw MXD and TRW data as well as the climate response. We considered MJJA temperature extremes (warm and cold) as well as larch budmoth (LBM) outbreaks to assess the response to and recovery from extreme events. Superposed epoch analysis (SEA, Panofsky and Brier, 1958) reveals the mean MXD and TRW deviations during the extreme year (year 0) and 5 years after, expressed as anomalies with respect to the mean of the 5 years preceding the event (years −5 to −1). We studied the six warmest and coldest summers and six LBM outbreak events corresponding to the LBM outbreak frequency (Baltensweiler and Rubli, 1999) during the common period of the chronologies. According to Baltensweiler and Rubli (1999), the years with heaviest LBM-induced discoloration are 1937, 1945, 1955, 1963, 1972 and 1981 for the Valais region. Within this region, the intensity of LBM outbreaks can vary with +/- 1 year, so that the heaviest outbreak might not exactly match the actual heaviest outbreak year in the Simplon valley but still this is the best available approximation. Five of the warmest summers since the onset of the E-OBS data in 1920 cluster after the year 2000. To reduce the overlap of superposed epochs we exclude temperature data after 2004. Thus, we considered 2003, 1998, 1947, 2001, 1994 and 1952 as warmest MJJA and 1978, 1954, 1980, 1939, 1940 and 1984 as coldest MJJA (sequentially sorted).

3. Results and discussion

3.1. Raw data comparison

Both raw MXD and TRW values generally decrease with elevation (Figs. 2a and S1a). For the overall MXD dataset 88% of the variance between the site median raw values can be explained by elevation. With 63% of explained variance this pattern is less clear for TRW as N15 seems to be an outlier among the raw TRW data. For MXD the variance

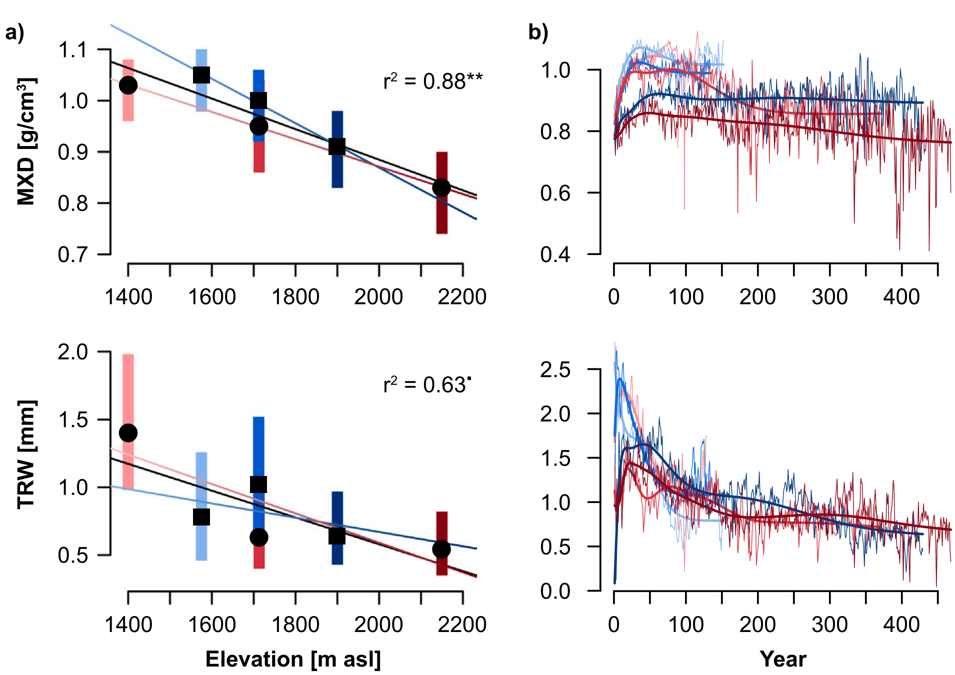

Fig. 2. Raw MXD and TRW data. a) Data is shown as a function of elevation. Bars represent the 25th to 75th percentiles and black signatures the respective medians of all measured rings. Squares represent north-facing slopes, circles south-facing slopes. Lines represent regression models for south- in red and north-facing slopes in blue and in black for the whole dataset, also r^2 is for the whole dataset (** = $p < 0.01$, • = $p < 0.1$). b) Cambial age aligned mean curves (regional curves). Colour code as in Fig. 1b.

of all measured raw values within a site is very low without any changes with elevation (see also Table 1). Considerably higher is the variance of raw TRW values, particularly at lower sites. It is common knowledge that ring widths decrease by getting closer to tree line (Hartl et al., 2021 and references there) while such patterns were not systematically observed for MXD yet. There are two studies, initially considering elevation effects on MXD (see Zhang et al., 2015 and Klippel et al., 2020) but also here a direct comparison with TRW data is lacking. In our study, it seems that the slope of decreasing MXD values is steeper for north-facing compared to south-facing sites. We, however, cannot prove this and refrain from declaring this as general statement because our network still does not comprise enough datapoints and the elevational gradient covered for south- and north-facing sites varies fundamentally.

This general pattern of decreasing values with elevation is also visible by considering the age aligned data for MXD but for TRW it is less clear (Figs. 2b and S1a). TRW is much more dependent on tree age than MXD with higher values and stronger variance for trees < ~170 years old (Fig. S1b). These fundamental level offsets of raw data from different elevations can have a crucial impact when RCS detrending is applied for a temperature reconstruction. It is generally accepted that RCS detrending is the best choice for temperature reconstructions as this detrending technique retains low-frequency signals which is not the case for individual series detrending. However, this advantage is at the same time the most tricky and influential factor with this technique: With RCS, tree-ring series of one site are aligned by cambial age. Then, the site-specific mean curve of all age-aligned series is calculated and a smoothed form of it (the so-called regional curve as shown in Fig. 2b) is subtracted from the single series before they are eventually dated back to calendar years (see Esper et al., 2003 for details). This means that the raw density and growth rates are substantial and strongly impacting. They are determining the index level after detrending with RCS. If a regional curve is produced from trees growing in a "wrong" region or site and finally would be combined with material from another growth environment as e.g. different elevational belt, this would result in an inappropriate detrending and biased temperature estimates (see Düthorn et al., 2013, 2015, Hartl et al., 2021 and Zhang et al., 2015). This means that it is of high importance to know the origin of wood from historical buildings for example and detrend such series with living tree material from the correct elevation. Despite of that and focussing back on the comparison of MXD and TRW data, it is obvious that the regional curves of the MXD data have level offsets. In accordance with the temperature lapse rate, the mean level of MXD is decreasing with increasing elevation. The regional curves from different elevations share a synchronous pattern of increasing values in the first 50 years (only S17 is deviating from that) and +/- no distinct fluctuations afterwards. The systematic level offset can be removed by a mean adjustment (Römer et al., 2021; Zhang et al., 2015) allowing the application of a single regional curve in the RCS detrending. The TRW age trend is much more complex and variable with strong and asynchronous fluctuations among the sites meaning that other disturbance factors have stronger effects on TRW than MXD so that MXD data is less biased and more reliable when focusing on the climatic signal in tree-ring data.

3.2. Changing covariance with elevation and between tree-ring parameters

As mentioned above, the Simplon valley offers great potential for a temperature reconstruction as historical material, spanning more than the past millennium, is available from buildings at higher elevations (Riechelmann et al., 2020). We thus focus on RCS detrended data as this would be the favourable detrending technique for such a purpose. However, we additionally consider 30-yr spline detrended data for the covariance analysis in the high-frequency domain. We found that covariance among chronologies increases with elevation within a parameter with highest correlations among higher but lower correlations among lower elevation sites (Fig. 3). This is true in the high as well as low frequency domain but also for the across parameter correlation which is higher in the higher elevations. Correlation coefficients between TRW and MXD RCS chronologies are very high with r > 0.7–0.77 for all sites above N17 (i.e., S17, N19, S21) but very low with r = 0.19 for the S14 site. For the 30-yr spline detrended chronologies, the correlation between parameters is consistently lower with r ranging between 0.56 and 0.67 for sites > N17 and there is no relationship between TRW and MXD for the lowest site S14 (r = −0.01). This fact is also an important information for MXD measurements in the lab itself because TRW chronologies are frequently used as reference for cross-dating the MXD series. Based on our results a correlation between TRW and MXD from *L. decidua* trees can only be expected for higher elevation sites in the European Alps. Björklund et al. (2019) found for raw Scots pine data from Scandinavia, that TRW and MXD are correlated but rather meaning that MXD data might not be as reliable when widths are narrow but this is rather connected to resolution issues. We here refer to detrended

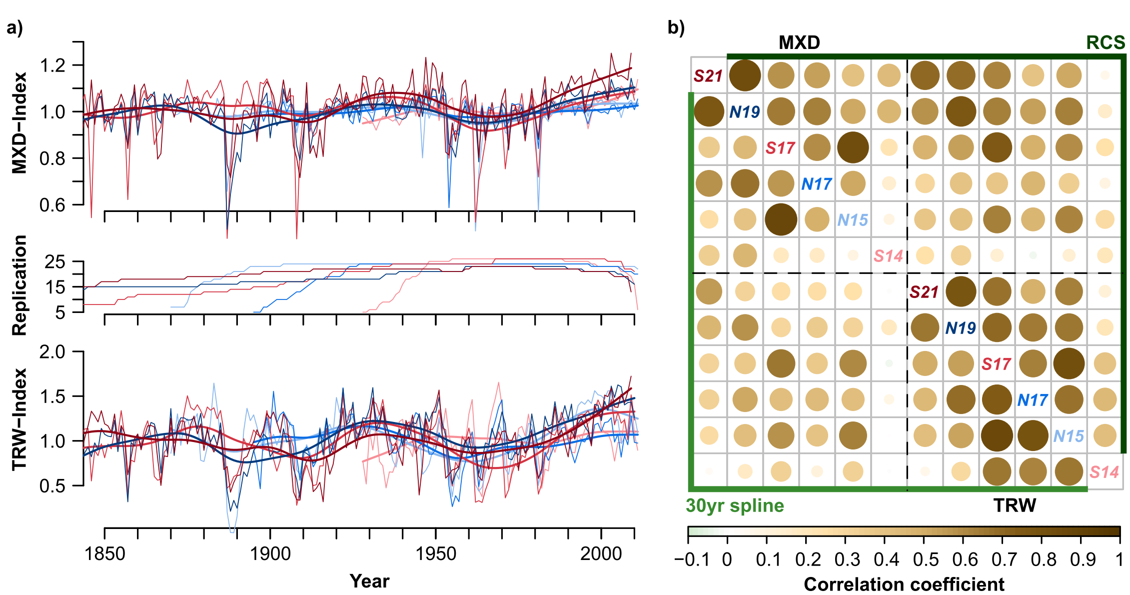

Fig. 3. a) RCS detrended MXD and TRW chronologies with their replication and b) the respective correlation matrix for RCS and 30 yr spline detrended chronologies for the 1928–2009 common period.

chronologies showing that the correlations between MXD and TRW data changes with elevation.

3.3. Climate signals inherent to MXD and TRW data at different elevations

Monthly climate response analysis revealed that particularly temperature has an influence on both MXD and TRW while precipitation seems less important (Figs. S2 and S3) for *L. decidua* in the European Alps. Highest and significant ($p < 0.05$) correlations are reached with RCS chronologies and during summer months. Therefore we focus on seasonal means (MJJ = May/June/July, JJA = June/July/August, and MJJA) and RCS chronologies. The patterns as described below are, however, very similar with 30-yr spline detrended data but with much lower (and frequently insignificant) correlation coefficients (see Figs. S3 and S4).

The elevation gradient of the temperature signal inherent to the chronologies is less pronounced for MXD compared to TRW data (Fig. 4). Generally highest correlations are reached with JJA and/or MJJA temperature data, thus representing the most important months for ring formation. Greatest summer temperature signals are reached with MXD data and at the high elevation sites ($r = 0.68–0.71$). Even the low elevation site S14 still shows high temperature signals with $r = 0.60$ (MJJA). The north-exposed sites have an elevation dependent climate response with a very steep slope, while on the south-exposed slope the medium elevation site has the weakest climate signal. Therefore the overall regression model is insignificant and elevation explains only 14% (for MJJ) to 31% (for JJA) of the variance (see Fig. 4a). It is unclear whether the gradient is obscured by too high correlations at site S14 or too low correlations at the sites N15, N17 and S17. The latter is more likely as will be discussed later but a final conclusion would need further sampling and measurements. The correlation of the MXD chronology including all series from six sites is very high with $r = 0.61$ (MJJ) and 0.65 (MJJA), exceeding the TRW signals even from highest elevations. However, by considering the TRW data (Fig. 4b), a very typical pattern of increased temperature signals with increasing elevation can be observed. Highest and significant correlations are reached at the two high elevation sites ($r = 0.56–0.58$) and lowest insignificant correlation for the lowest site ($r = 0.02–0.12$). This strong dependence to elevation is very well explained by a linear regression model with r^2 ranging from 0.64 (MJJA) to 0.70 (MJJ). These patterns were repeatedly observed by various studies also for *L. decidua* (Hartl-Meier et al., 2014b, 2017; Riechelmann et al., 2020) as well as for other tree species (Dittmar and Elling, 1999; Hartl-Meier et al., 2014a, 2014b; Hartl et al., 2021). The slopes of the regression models are very similar for both south- and north-facing slopes. The correlation coefficient of the TRW chronology including the overall dataset is substantially lower compared to the MXD coefficient with $r = 0.46$ (JJA) and $r = 0.50$ (MJJA). In general, the MXD chronologies show higher correlations with temperature compared to their TRW counterpart, except for the N15 site.

When considering the spatial correlations of RCS chronologies, it is confirmed that MXD chronologies comprise stronger temperature signals than TRW (Fig. 5). Only at site N15 TRW reveals stronger and spatially wider signals. The TRW chronology from site S14 shows no correlation in space at all. In general, Büntgen et al. (2010) found similar spatial correlation patterns of Alpine MXD data. If MXD data even from low elevation sites are able to provide larger scale information about temperature variability, it is likely possible to produce temperature reconstructions with wood grown in an unknown elevation and extracted from historical buildings. This fact is particularly emphasised by the high correlation of the low elevation site as well as by the correlation of the overall chronology. However, as mentioned above, and to draw overall conclusions this statement would need further approval using additional data and potentially by also extending the elevational transect.

3.4. Depiction of extreme events in MXD and TRW chronologies

Next to the long-term correlation with temperature, parameter performance is also determined by the response to extreme climatic events. We thus selected the coldest and warmest years in the chronologies' common period and performed a SEA (Fig. 6a and b). All MXD chronologies show increased values during the selected years with highest summer temperatures but do not capture the full actual warmth (black

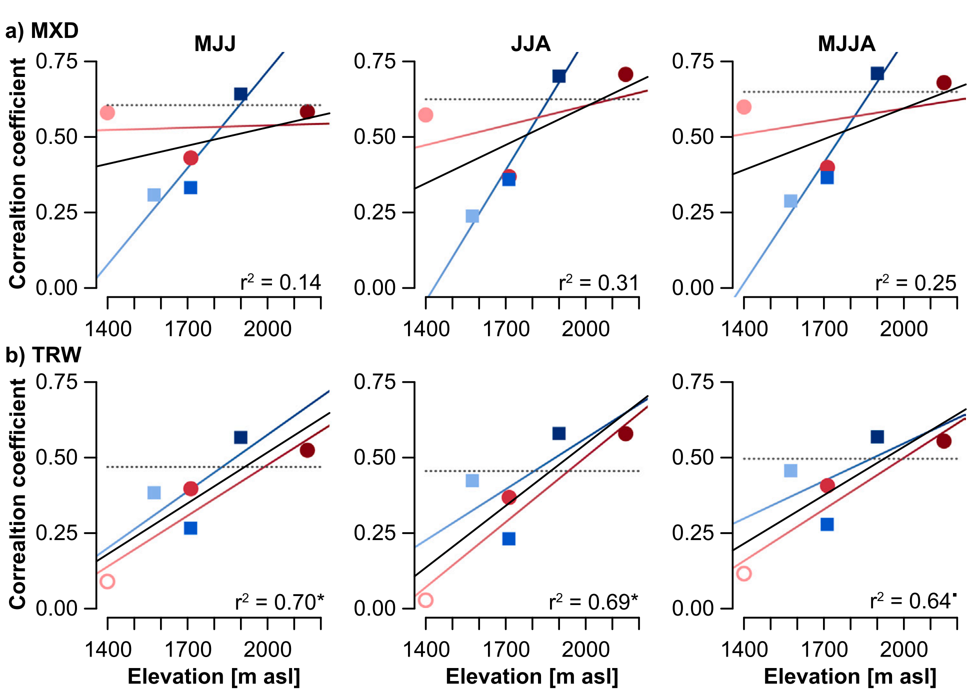

Fig. 4. Seasonal temperature responses of RCS detrended a) MXD and b) TRW chronologies with EOBS climate data for the 1928–2009 period. Filled symbols are significant at $p < 0.05$. The dotted line represents the correlation coefficient of the chronology including the overall dataset independent of elevation. Lines represent regression models for south in red and north-facing slopes in blue and in black for the whole dataset, also r^2 is for the whole dataset. * = $p < 0.05$, • = $p < 0.1$.

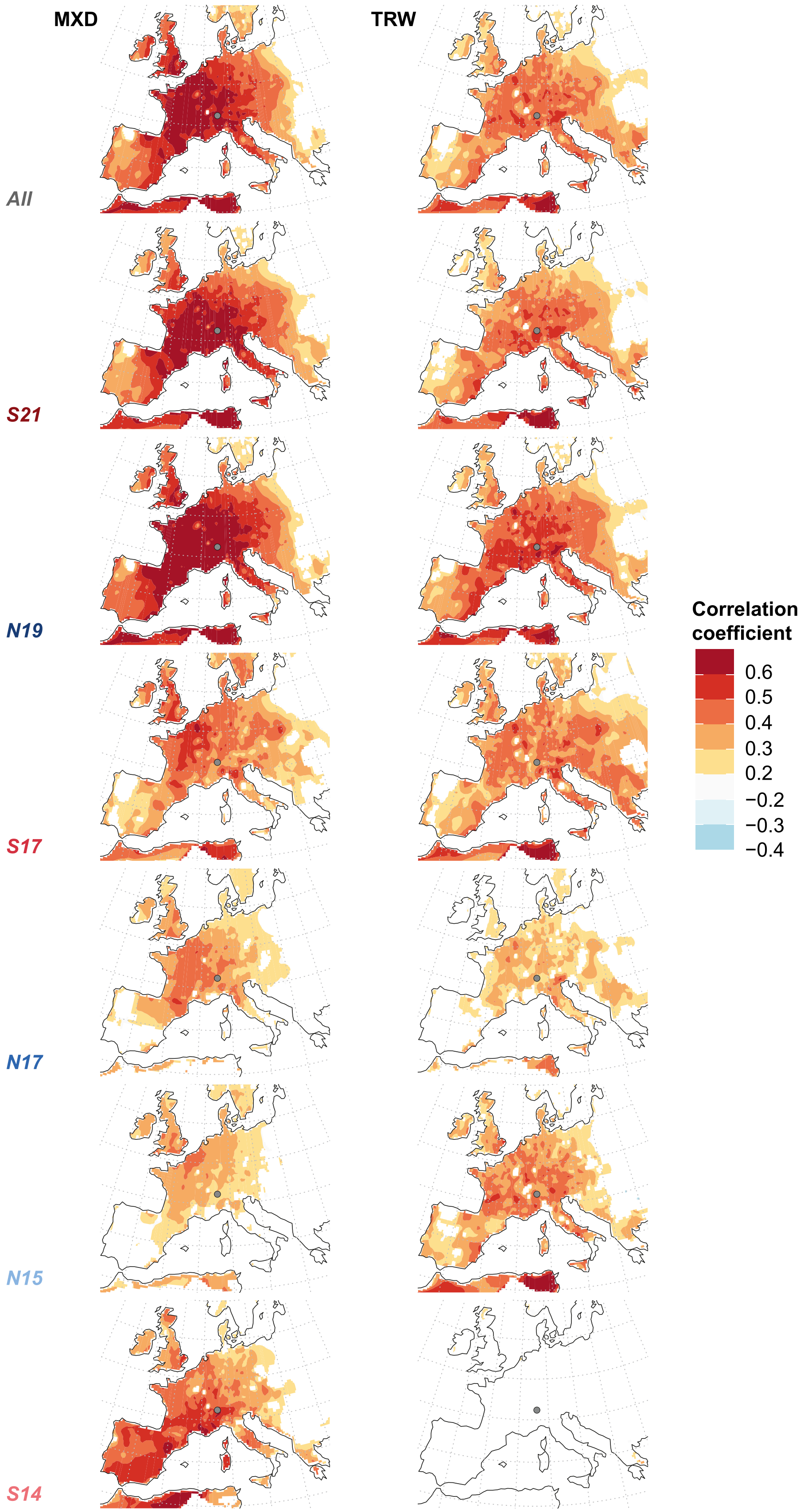

Fig. 5. Spatial MJJA temperature responses of RCS detrended MXD and TRW chronologies with EOBS climate data for the 1928–2009 period.

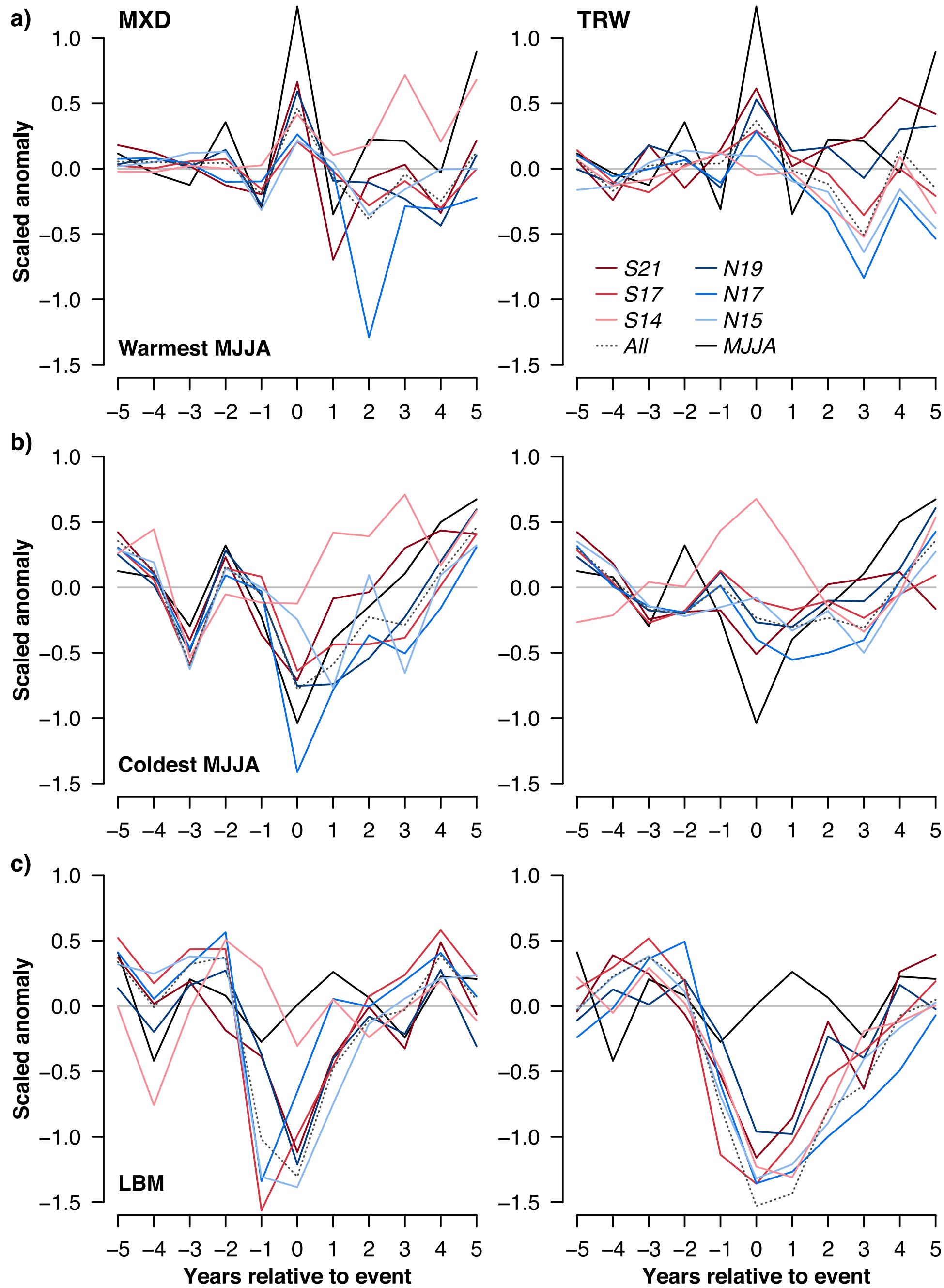

Fig. 6. Superposed epoch analysis of MXD and TRW chronologies together with the MJJA temperature record for a) the warmest and b) coldest MJJA seasons as well as for c) LBM mass outbreaks.

line). However, MXD chronologies still better represent the temperature record than TRW (Fig. 6a). Focusing on the cold events it is very obvious that particularly low temperatures are best represented with MXD data (Fig. 6b). Almost all chronologies follow (except from S14 and N15) closely the temperature record during these years and specifically the north-exposed sites track the cold events very well. Most strikingly the TRW data cannot represent these cold events, a fact which was not observed before and representing new and important knowledge for dendroclimatology. The S14 site even shows higher growth during these years. However, *L. decidua* trees in the Western Alps are not only influenced by climate but also larch budmoth mass outbreaks (Büntgen et al., 2009, 2020; Esper et al., 2007; Hartl-Meier et al., 2017). The larvae of this insect are feeding the needles of *L. decidua* trees, leading to reduced radial growth of the tree. Due to cyclic mass outbreaks every 8–10 years, this insect triggers a very typical and distinct pattern in the tree-rings (Fig. 6c). This pattern is very obvious in all our MXD chronologies showing declining values in year 0 or even year −1 which are obviously not connected to temperature changes (see black line again). It is not surprising that the strongest decline varies among the sites as we here selected the years with heaviest outbreaks after Baltensweiler and Rubli (1999) for the greater region, i.e. the whole Valais. It is known that LBM mass outbreaks appear like travelling waves across the whole European Alps from south-west to north-east (Bjørnstad et al., 2002) and we have to point out that outbreak patterns can also vary on much smaller spatial scale, even within a valley (Baltensweiler and Rubli, 1999). The duration of LBM-induced MXD declines is up to two years with a quick recovery to average density values afterwards. TRW shows distinct growth declines during those years, too. However, the recovery of growth takes much longer, up to 4 years. This behaviour is in line with previous findings (Battipaglia et al., 2014; Hartl-Meier et al., 2017). It is well known that memory effects are more pronounced in TRW compared to MXD (Esper et al., 2015). The longer lasting effects of LBM events, i.e. narrow rings which strongly influence correlations, seems to be causative for the higher Rbar values we found in the TRW compared to MXD data (Table 1). Besides that, the optimal outbreak zone for LBM is estimated at 1700 and 2000 m asl (Baltensweiler et al., 2008; Hartl-Meier et al., 2017; Johnson et al., 2010). Our results also suggest that the medium elevations were affected most by LBM explaining the weaker temperature signal in MXD data from N15, N17 and S17. For temperature reconstructions based on *L. decidua* trees it is thus important to control for potential effects of LBM outbreaks, for example using a non-host species.

4. Conclusion

We performed a detailed comparison of TRW and MXD data and analysed the effects of elevation and site aspect on both parameters. We found a systematic imprint of elevation and aspect in raw MXD data, independent of the age structure of underlying samples. After detrending, the chronologies revealed highest signal-to-noise ratios for MXD and for the high-elevation sites, confirming that tree growth is most strongly controlled by climate towards the elevational tree line. The superior performance of MXD is emphasised with the correlation analysis of temperature signals. Although the elevation gradient in growth/climate relationships is more clearly depicted in TRW data, the overall signal strength is higher in MXD. The climate signal of a combined chronology including MXD series from all elevations is even stronger compared to the high elevation TRW site(s). This means that material with unknown origin might affect a temperature reconstruction, but the elevational differences are more significant in TRW data, and the inclusion of data from unknown location can therefore bias TRW chronologies more than MXD chronologies. An RCS detrending with MXD data including historical wood should only be employed after a careful investigation of structural offsets between the regional curves from living and historical wood material. The obscured elevation gradient in MXD climate signals is likely related to the impact of LBM outbreaks. We also want to point out that our results can only be applied for this species, i.e. *L. decidua* and this environment, i.e. the European Alps. The impact of elevation and slope aspect should be considered for other tree species and in other environments, for example in the Mediterranean. The existing chronologies from this region are often produced from relict in situ wood. But historical buildings and archaeological sites provide great potential to extend these chronologies even further back in time and increase replication, leading to even more robust chronologies and temperature estimates.

Declaration of Competing Interest

None declared.

Acknowledgements

We are grateful to the forest district Simplon-South and especially M. Gerold for the permission to sample trees in Simplon valley. We thank Robin Schulz, Lara Meurer and Jannes Fischer for help in the laboratory. CH was supported by the German Research Foundation [Grant number HA 8048/1-1]. UB and JE received funding from SustES: Adaptation strategies for sustainable ecosystem services and food security under adverse environmental conditions (CZ.02.1.01/0.0/0.0/16_019/0000797), and the ERC project MONOSTAR (AdG 882727).

Appendix A. Supplementary material

Supplementary data associated with this article can be found in the online version at doi:10.1016/j.dendro.2022.125958.

References

Baltensweiler, W., Rubli, D., 1999. Dispersal: an important driving force of the cyclic population dynamics of the larch bud moth, Zeiraphera diniana Gn. For. Snow Landsc. Res. 74, 3–153.

Baltensweiler, W., Weber, U.M., Cherubini, P., 2008. Tracing the influence of larch-bud-moth insect outbreaks and weather conditions on larch tree-ring growth in Engadine (Switzerland). Oikos 117, 161–172. https://doi.org/10.1111/j.2007.0030-1299.16117.x.

Battipaglia, G., Büntgen, U., McCloskey, S.P.J., Blarquez, O., Denis, N., Paradis, L., Brossier, B., Fournier, T., Carcaillet, C., 2014. Long-term effects of climate and land-use change on larch budmoth outbreaks in the French Alps. Clim. Res. 62, 1–14. https://doi.org/10.3354/cr01251.

Björklund, J., Arx, G., Nievergelt, D., Wilson, R., Van den Bulcke, J., Günther, B., Loader, N.J., Rydval, M., Fonti, P., Scharnweber, T., Andreu-Hayles, L., Büntgen, U., D'Arrigo, R., Davi, N., De Mil, T., Esper, J., Gärtner, H., Geary, J., Gunnarson, B.E., Hartl, C., Hevia, A., Song, H., Janecka, K., Kaczka, R.J., Kirdyanov, A.V., Kochbeck, M., Liu, Y., Meko, M., Mundo, I., Nicolussi, K., Oelkers, R., Pichler, T., Sánchez-Salguero, R., Schneider, L., Schweingruber, F., Timonen, M., Trouet, V., Van Acker, J., Verstege, A., Villalba, R., Wilmking, M., Frank, D., 2019. Scientific merits and analytical challenges of tree-ring densitometry. Rev. Geophys. 57, 1224–1264. https://doi.org/10.1029/2019RG000642.

Bjørnstad, O.N., Peltonen, M., Liebhold, A.M., Baltensweiler, W., 2002. Waves of larch budmoth outbreaks in the European Alps. Science 298, 1020–1023. https://doi.org/10.1126/science.1075182.

Büntgen, U., Esper, J., Frank, D., Nicolussi, K., Schmidhalter, M., 2005. A 1052-year tree-ring proxy for Alpine summer temperatures. Clim. Dyn. 25, 141–153. https://doi.org/10.1007/s00382-005-0028-1.

Büntgen, U., Bellwald, I., Kalbermatten, H., Schmidhalter, M., Frank, D.C., Freund, H., Bellwald, W., Neuwirth, B., Nüsser, M., Esper, J., 2006. 700 years of settlement and building history in the Loetschental, Switzerland. Erdkunde 2, 96–112. https://doi.org/10.3112/erdkunde.2006.02.02.

Büntgen, U., Frank, D., Liebhold, A.M., Johnson, D.M., Carrer, M., Urbinati, C., Grabner, M., Nicolussi, K., Levanič, T., Esper, J., 2009. Three centuries of insect outbreaks across the European Alps. New Phytol. 182, 929–941. https://doi.org/10.1111/j.1469-8137.2009.02825.x.

Büntgen, U., Franke, J., Frank, D., Wilson, R.J.S., González-Rouco, J.F., Esper, J., 2010. Assessing the spatial signature of European climate reconstructions. Clim. Res. 41, 125–130. https://doi.org/10.3354/cr00848.

Büntgen, U., Kyncl, T., Ginzler, C., Jacks, D.S., Esper, J., Tegel, W., Heußner, K.-U., 2013. Filling the Eastern European gap in millennium-long temperature reconstructions. Proc. Natl. Acad. Sci. 110, 1773–1778. https://doi.org/10.1073/pnas.1211485110.

Büntgen, U., Krusic, P.J., Verstege, A., Sangüesa-Barreda, G., Wagner, S., Camarero, J.J., Ljungqvist, F.C., Zorita, E., Oppenheimer, C., Konter, O., Tegel, W., Gärtner, H., Cherubini, P., Reinig, F., Esper, J., 2017. New tree-ring evidence from the pyrenees reveals western Mediterranean climate variability since medieval times. J. Clim. 30, 5295–5318. https://doi.org/10.1175/JCLI-D-16-0526.1.

Büntgen, U., Liebhold, A., Nievergelt, D., Wermelinger, B., Roques, A., Reinig, F., Krusic, P.J., Piermattei, A., Egli, S., Cherubini, P., Esper, J., 2020. Return of the moth: rethinking the effect of climate on insect outbreaks. Oecologia 192, 543–552. https://doi.org/10.1007/s00442-019-04585-9.

Cook, E.R., Peters, K., 1981. The smoothing spline: a new approach to standardizing forest interior tree-ring width series for dendroclimatic studies. Tree-Ring Bull. 41, 45–55.

Cornes, R.C., van der Schrier, G., van den Besselaar, E.J.M., Jones, P.D., 2018. An ensemble version of the E-OBS temperature and precipitation data sets. J. Geophys. Res. Atmos. 123, 9391–9409. https://doi.org/10.1029/2017JD028200.

Dittmar, C., Elling, W., 1999. Jahrringbreite von Fichte und Buche in Abhängigkeit von Witterung und Höhenlage. Forstwiss. Cent. 118, 251–270.

Duffy, J.E., McCarroll, D., Loader, N.J., Young, G.H.F., Davies, D., Miles, D., Bronk Ramsey, C., 2019. Absence of age-related trends in stable oxygen isotope ratios from oak tree rings. Glob. Biogeochem. Cycles 33, 841–848. https://doi.org/10.1029/2019GB006195.

Düthorn, E., Holzkämper, S., Timonen, M., Esper, J., 2013. Influence of micro-site conditions on tree-ring climate signals and trends in central and northern Sweden. Trees Struct. Funct. 27, 1395–1404. https://doi.org/10.1007/s00468-013-0887-8.

Düthorn, E., Schneider, L., Konter, O., Schön, P., Timonen, M., Esper, J., 2015. On the hidden significance of differing micro-sites on tree-ring based climate reconstructions. Silva Fenn. 49. https://doi.org/10.14214/sf.1220.

Esper, J., Cook, E.R., Krusic, P.J., Peters, K., 2003. Tests of the RCS method for preserving low-frequency variability in long tree-ring chronologies. Tree-Ring Res. 59, 81–98.

Esper, J., Büntgen, U., Frank, D., Nievergelt, D., Liebhold, A.M., 2007. 1200 years of regular outbreaks in alpine insects. Proc. R. Soc. B Biol. Sci. 274, 671–679. https://doi.org/10.1098/rspb.2006.0191.

Esper, J., Frank, D., Timonen, M., Zorita, E., Wilson, R.J.S., Luterbacher, J., Holzkämper, S., Fischer, N., Wagner, S., Nievergelt, D., Verstege, A., Büntgen, U., 2012. Orbital forcing of tree-ring data. Nat. Clim. Change 2, 862–866. https://doi.org/10.1038/nclimate1589.

Esper, J., Schneider, L., Smerdon, J.E., Schöne, B.R., Büntgen, U., 2015. Signals and memory in tree-ring width and density data. Dendrochronologia 35, 62–70. https://doi.org/10.1016/j.dendro.2015.07.001.

Esper, J., Krusic, P.J., Ljungqvist, F.C., Luterbacher, J., Carrer, M., Cook, E.R., Davi, N.K., Hartl-Meier, C., Kirdyanov, A.V., Konter, O., Myglan, V.S., Timonen, M., Treydte, K., Trouet, V., Villalba, R., Yang, B., Büntgen, U., 2016. Ranking of tree-ring based temperature reconstructions of the past millennium. Quat. Sci. Rev. 145, 134–151. https://doi.org/10.1016/j.quascirev.2016.05.009.

Esper, J., Klippel, L., Krusic, P.J., Konter, O., Raible, C.C., Xoplaki, E., Luterbacher, J., Büntgen, U., 2020a. Eastern Mediterranean summer temperatures since 730 CE from Mt. Smolikas tree-ring densities. Clim. Dyn. 54, 1367–1382. https://doi.org/10.1007/s00382-019-05063-x.

Esper, J., Hartl, C., Tejedor, E., de Luis, M., Günther, B., Büntgen, U., 2020b. High-resolution temperature variability reconstructed from black pine tree ring densities in Southern Spain. Atmosphere 11, 748. https://doi.org/10.3390/atmos11070748.

Frank, D., Esper, J., 2005. Characterization and climate response patterns of a high-elevation, multi-species tree-ring network in the European Alps. Dendrochronologia 22, 107–121. https://doi.org/10.1016/j.dendro.2005.02.004.

Hartl, C., Düthorn, E., Tejedor, E., Kirchhefer, A.J., Timonen, M., Holzkämper, S., Büntgen, U., Esper, J., 2021. Micro-site conditions affect Fennoscandian forest growth. Dendrochronologia 65, 125787. https://doi.org/10.1016/j.dendro.2020.125787.

Hartl-Meier, C., Dittmar, C., Zang, C., Rothe, A., 2014a. Mountain forest growth response to climate change in the Northern Limestone Alps. Trees Struct. Funct. 28, 819–829. https://doi.org/10.1007/s00468-014-0994-1.

Hartl-Meier, C., Zang, C., Dittmar, C., Esper, J., Göttlein, A., Rothe, A., 2014b. Vulnerability of Norway spruce to climate change in mountain forests of the European Alps. Clim. Res. 60, 119–132. https://doi.org/10.3354/cr01226.

Hartl-Meier, C., Zang, C., Büntgen, U., Esper, J., Rothe, A., Göttlein, A., Dirnböck, T., Treydte, K., 2015. Uniform climate sensitivity in tree-ring stable isotopes across species and sites in a mid-latitude temperate forest. Tree Physiol. 35, 4–15. https://doi.org/10.1093/treephys/tpu096.

Hartl-Meier, C., Esper, J., Liebhold, A., Konter, O., Rothe, A., Büntgen, U., 2017. Effects of host abundance on larch budmoth outbreaks in the European Alps. Agric. For. Entomol. https://doi.org/10.1111/afe.12216.

Johnson, D.M., Büntgen, U., Frank, D., Kausrud, K., Haynes, K.J., Liebhold, A.M., Esper, J., Stenseth, N.C., 2010. Climatic warming disrupts recurrent Alpine insect outbreaks. Proc. Natl. Acad. Sci. 107, 20576–20581. https://doi.org/10.1073/pnas.1010270107.

Klippel, L., Krusic, P.J., Konter, O., St. George, S., Trouet, V., Esper, J., 2019. A 1200+ year reconstruction of temperature extremes for the northeastern Mediterranean region. Int. J. Clim. 39, 2336–2350. https://doi.org/10.1002/joc.5955.

Klippel, L., Büntgen, U., Konter, O., Kyncl, T., Esper, J., 2020. Climate sensitivity of high- and low-elevation Larix decidua MXD chronologies from the Tatra Mountains. Dendrochronologia 60, 125674. https://doi.org/10.1016/j.dendro.2020.125674.

Konter, O., Krusic, P.J., Trouet, V., Esper, J., 2017. Meet Adonis, Europe's oldest dendrochronologically dated tree. Dendrochronologia 42, 12. https://doi.org/10.1016/j.dendro.2016.12.001.

Luterbacher, J., Werner, J.P., Smerdon, J.E., Fernández-Donado, L., González-Rouco, J. F., Barriopedro, D., Ljungqvist, F.C., Büntgen, U., Zorita, E., Wagner, S., Esper, J., McCarroll, D., Toreti, A., Frank, D., Jungclaus, J.H., Barriendos, M., Bertolin, C., Bothe, O., Brázdil, R., Camuffo, D., Dobrovolný, P., Gagen, M.H., García-Bustamante, E., Ge, Q., Gómez-Navarro, J.J., Guiot, J., Hao, Z., Hegerl, G.C., Holmgren, K., Klimenko, V.V., Martín-Chivelet, J., Pfister, C., Roberts, N., Schindler, A., Schurer, A.P., Solomina, O., Gunten, L., von Wahl, E.R., Wanner, H., Wetter, O., Xoplaki, E., Yuan, N., Zanchettin, D., Zhang, H., Zerefos, C., 2016. European summer temperatures since Roman times. Environ. Res. Lett. 11, 024001 https://doi.org/10.1088/1748-9326/11/2/024001.

Mosteller, F., Tukey, J.W., 1977. Data Analysis and Regression: A Second Course in Statistics, Addison-Wesley Series in Behavioral Science. Quantitative Methods. Addison-Wesley Pub. Co., Reading, Massachusetts.

Panofsky, H.A., Brier, G.W., 1958. Some Applications of Statistics to Meteorology. University Park, Pennsylvania.

Piovesan, G., Biondi, F., Baliva, M., Presutti Saba, E., Calcagnile, L., Quarta, G., D'Elia, M., De Vivo, G., Schettino, A., Di Filippo, A., 2018. The oldest dated tree of Europe lives in the wild Pollino massif: *Italus*, a strip-bark Heldreich's pine. Ecology 99, 1682–1684. https://doi.org/10.1002/ecy.2231.

Riechelmann, D., Hartl, C., Esper, J., 2020. The effect of provenance of historical timber on tree-ring based temperature reconstructions in the Western Central Alps. iForest 13, 351–359. https://doi.org/10.3832/ifor3412-013.

Römer, P., Hartl, C., Schneider, L., Bräuning, A., Szymczak, S., Huneau, F., Lebre, S., Reinig, F., Büntgen, U., Esper, J., 2021. Reduced temperature sensitivity of maximum latewood density formation in high-elevation corsican pines under recent warming. Atmosphere 12, 804. https://doi.org/10.3390/atmos12070804.

Schweingruber, F.H., Bartholin, T., Schär, E., Briffa, K.R., 1988. Radiodensitometric-dendroclimatological conifer chronologies from Lapland (Scandinavia) and the Alps (Switzerland). Boreas 17, 559–566. https://doi.org/10.1111/j.1502-3885.1988.tb00569.x.

Zhang, P., Björklund, J., Linderholm, H.W., 2015. The influence of elevational differences in absolute maximum density values on regional climate reconstructions. Trees Struct. Funct. 29, 1259–1271. https://doi.org/10.1007/s00468-015-1205-4.